

Data-Assimilation in Shallow Water Flows

Introduction

Given the recent surge in interest in data assimilation strategies in oceanography [1, 2, 3, 4, 5], it is interesting then to ask how these approaches might be used to incorporate data into surface wave estimation. While the inclusion of nonlinearity in surface-wave modeling was traditionally complicated due to the need to solve a nonlinear free-boundary value problem, through the work of [6, 7, 8, 9, 10, 11] and others, it is now quite feasible to compute fully nonlinear solutions to the surface-wave problem to high accuracy. Likewise, given the recent work of [12], there is an increased interest in better understanding how to improve the assimilation of surface wave data into more complicated water-wave models.

Thus, in this paper, we explore the use of ensemble Kalman filters [13] as a means of incorporating data into the modeling of free surface waves. While not as sophisticated as more general Bayesian assimilation schemes, see [3, 5] for example, Kalman filters are a well understood and highly used means of data assimilation in oceanography [13] and meteorology [14]. As we show, we can readily use ensemble Kalman filters to incorporate both Eulerian measurements, corresponding to measurements made by buoys tethered to sea-floor pressure plates, and Lagrangian measurements, corresponding to untethered, freely floating buoys.

Throughout the remainder of this paper, we use as a model for a freely evolving ocean surface the free boundary value problem

$$\begin{aligned}\Delta\phi &= 0, & -h < z < \eta(x, t) \\ \phi_z &= 0, & z = -h \\ \eta_t + \eta_x\phi_x - \phi_z &= 0, & z = \eta(x, t) \\ \phi_t + \frac{1}{2}|\nabla\phi|^2 + g\eta &= 0, & z = \eta(x, t),\end{aligned}$$

where $\phi(x, z, t)$ is the velocity potential and the free fluid surface is given by $z = \eta(x, t)$. As pointed out in [15] and [16], the AFM/DNO method is best suited to shallow water environments. We therefore introduce the following non-dimensionalizations

$$\tilde{x} = \frac{x}{\lambda}, \quad \tilde{z} = \frac{z}{h}, \quad \tilde{t} = \frac{\sqrt{gh}}{\lambda}t, \quad \eta = a\tilde{\eta}, \quad \phi = \frac{ag\lambda}{\sqrt{gh}}\tilde{\phi},$$

and non-dimensional parameters

$$\epsilon = \frac{a}{h}, \quad \mu = \frac{h}{\lambda},$$

whereby we can, after dropping tildes, rewrite the free surface problem in the non-dimesnional form

$$\begin{aligned} \phi_{xx} + \frac{1}{\mu^2} \phi_{zz} &= 0, \quad -1 < z < \epsilon\eta(x, t), \\ \phi_z &= 0, \quad z = -1, \\ \eta_t + \epsilon\eta_x \phi_x - \frac{1}{\mu^2} \phi_z &= 0, \quad z = \epsilon\eta(x, t), \\ \phi_t + \frac{\epsilon}{2} \left(\phi_x^2 + \frac{1}{\mu^2} \phi_z^2 \right) + \eta &= 0, \quad z = \epsilon\eta(x, t). \end{aligned}$$

Here, ϵ is a measure of the characteristic wave amplitude, a , to the quiescent fluid depth, h , while μ is a measure of the quiescent fluid depth to the characteristic wavelength, λ , of the free surface waves. We will describe the fluid as being ‘shallow-water’ when ϵ and μ are both small. For the purposes of this report, we will choose $\epsilon = .1$ and $\mu = \sqrt{\epsilon}$, which corresponds to looking at meter high waves over ten meters of fluid, with characteristic wavelengths then on the order of thirty meters. Our choice of $\mu = \sqrt{\epsilon}$ is the one used to derive the Korteweg–de Vries equation, which is a classic shallow water model. In the following, we look at an approach whereby the free boundary value problem above becomes a closed system in terms of the surface variables $\eta(x, t)$ and $q(x, t)$ where the surface potential $q(x, t)$ is defined to be

$$q(x, t) = \phi(x, \epsilon\eta(x, t), t),$$

AFM/DNO Method

The AFM/DNO method begins from an observation first made in [17] that one can readily show that

$$\eta_t = \phi_z - \eta_x \phi_x = \sqrt{1 + \epsilon^2 \mu^2 \eta_x^2} \partial_{\mathbf{n}} \phi,$$

where $\partial_{\mathbf{n}} \phi$ denotes the normal derivative of the velocity potential at the surface $z = \epsilon\eta(x, t)$. Then, following [17], we can define a Dirichlet-to-Neumann operator (DNO), say $G(\eta)$, whereby we can write

$$\sqrt{1 + \epsilon^2 \mu^2 \eta_x^2} \partial_{\mathbf{n}} \phi = G(\eta)q.$$

We can then derive the closed system of evolution equations for η and q of the form

$$\eta_t = G(\eta)q \tag{1}$$

$$q_t = -\eta - \frac{\epsilon}{2} q_x^2 + \frac{\epsilon \mu^2}{2} \frac{(G(\eta)q + \epsilon \eta_x q_x)^2}{1 + \epsilon^2 \mu^2 \eta_x^2} \tag{2}$$

Of course, to make this approach useful, one must determine a computable form of the DNO. To do so, following arguments in [6], we use the fact that G is an analytic function of η so that

$$G(\eta)q = \sum_{j=0}^M \epsilon^j G_j(\eta)q + \mathcal{O}(\epsilon^{M+1}).$$

While there are several ways to determine the terms in this expansion, we argue that using the AFM formulation of the free surface wave problem makes this process more straightforward than other approaches. Following then the results in [11], we derive the following integro-differential equation

$$\int_{-L}^L e^{-ikx} \left(\cosh(\mu \tilde{k}(1 + \epsilon\eta)) \eta_t + \frac{i q_x}{\mu} \sinh(\mu \tilde{k}(1 + \epsilon\eta)) \right) dx = 0, \quad \tilde{k} = \frac{\pi k}{L}.$$

Inserting the DNO expansion from above, expanding the hyperbolic trigonometric terms, and then matching powers of ϵ provides the following recursive formulas for the coefficients of the DNO, where for $j \geq 1$,

$$\widehat{(G_j q)}_k = - \sum_{m=0}^{j-1} \frac{(\mu \tilde{k})^{(j-m)}}{(j-m)!} L_{j-m} \left(\eta^{(j-m)} G_m q \right)_k - \frac{i}{\mu} \tilde{k}^j L_{j+1} \left(\eta^j q_x \right)_k, \quad (3)$$

with

$$\widehat{(G_0 q)}_k = \frac{\tilde{k}}{\mu} \tanh(\mu \tilde{k}) \hat{q}_k,$$

and

$$L_j(k) = \begin{cases} 1, & j \text{ even}, \\ \tanh(\mu \tilde{k}), & j \text{ odd}. \end{cases}$$

The Ensemble Kalman Filter

The Linear Kalman Filter

We briefly review the now classic and widely used linear Kalman filter before discussing its nonlinear variant, the ensemble Kalman filter. The linear Kalman filter supposes that some true state of a system, described by the time dependent N_m -dimensional vector at time t_n , say $x_n^{(tr)}$, is given via the model

$$x_n^{(tr)} = \mathcal{N} x_{n-1}^{(tr)} + \epsilon_{n-1}^{(m)},$$

where \mathcal{N} is a model matrix which attempts to transform the prior true state into the next true state. However, we suppose that the model is not complete to describe the true state, and that model deficiencies manifest themselves

via the error vector ϵ_{n-1} . The error vectors are assumed to consist of zero-mean Gaussian random variables with the further assumption that

$$\mathbb{E} \left[\epsilon_j^{(m)} \left(\epsilon_k^{(m)} \right)^T \right] = \delta_{jk} Q_k,$$

which is to say that the errors are uncorrelated in time, while at a given time step there is one covariance matrix to typefy the deviation among the model errors. Likewise, we suppose that at time t_n , we have an N_d -dimensional vector of measurements given by d_n which corresponds to the true state via the equation

$$d_n = H x_n^{(tr)} + \epsilon_n^{(d)},$$

where H is the measurment matrix and the errors in measurement are incorporated into the zero-mean, Gaussian vector $\epsilon_n^{(d)}$, which we further suppose satisfies the identity

$$\mathbb{E} \left[\epsilon_j^{(d)} \left(\epsilon_k^{(d)} \right)^T \right] = \delta_{jk} R_k, \quad \mathbb{E} \left[\epsilon_j^{(m)} \left(\epsilon_k^{(d)} \right)^T \right] = 0.$$

We now suppose that, in effect, we have no access to the true state. However, we suppose that at time t_n , through some mechanism, we have a N_m -dimensional *forecast*, say $x_n^{(f)}$. We can then define the error covariance matrix

$$P_n^{(f)} = \mathbb{E} \left[\left(x_n^{(f)} - x_n^{(tr)} \right) \left(x_n^{(f)} - x_n^{(tr)} \right)^T \right].$$

We then ask, given a forecast, can we incorporate the data in such a way to create a better estimate to the true state? To do this, we suppose that this better *analysis* state, say $x_n^{(a)}$ is given by

$$x_n^{(a)} = x_n^{(f)} + K_n (d_n - H x_n^{(f)}),$$

where the gain matrix K_n is chosen so as to minimize the trace of the affiliated error covariance matrix $P_n^{(a)}$ where

$$P_n^{(a)} = \mathbb{E} \left[\left(x_n^{(a)} - x_n^{(tr)} \right) \left(x_n^{(a)} - x_n^{(tr)} \right)^T \right].$$

Thus, the analysis vector represents the best estimate to the true state using the given forecast and measurements of the system. As can be shown, K_n is then given by

$$K_n = P_n^{(f)} H^T \left(H P_n^{(f)} H^T + R_n \right)^{-1}.$$

This optimization procedure likewise gives us the affiliated analysis error covariance matrix $P_n^{(a)}$ where

$$P_n^{(a)} = (I - K_n H) P_n^{(f)}.$$

At this point, we note that with a forecast estimate $x_n^{(f)}$ and error covariance matrix $P_n^{(f)}$, we were able to create a best estimate incorporating the data obtained via measurement to produce the analysis estimate $x_n^{(a)}$ with the corresponding error covariance matrix $P_n^{(a)}$. To go to the next time step then, we let

$$x_{n+1}^{(f)} = \mathcal{N}x_n^{(a)}, \quad P_{n+1}^{(f)} = \mathcal{N}P_n^{(a)}\mathcal{N}^T + Q_n.$$

Note the recursive structure of the Kalman filter, whereby information from only the immediately previous time-step is necessary to progress to the next time step.

The Ensemble Kalman Filter

As noted, the above process is well-defined when modeling linear systems. In the case though that the model is nonlinear, i.e.

$$x_n^{(tr)} = f\left(x_{n-1}^{(tr)}\right) + \epsilon_{n-1}^{(m)},$$

then more thought is necessary in order to perform the filtration. In particular, we see that the update step associated with generating the forecast error covariance matrix is no longer applicable. While one could replace M with linearizations around the computed analysis estimate, as in the Extended Kalman Filter, this has proved to be both computationally costly and unstable with respect to error.

Instead, we introduce the idea of an ensemble of say N_e forecasts in which now $x_n^{(f)}$ denotes an $N_m \times N_e$ matrix which generates the ensemble average, $\bar{x}_n^{(f)}$ where

$$\bar{x}_n^{(f)} = \frac{1}{N_e} \sum_{j=1}^{N_e} x_{n,j}^{(f)}.$$

Using this average as an approximation to the true state, we can likewise generate an estimate to the error covariance matrix $P_n^{(f)}$ via the formula

$$P_n^{(f)} \approx \frac{1}{N_e - 1} \sum_{j=1}^{N_e} \left(x_{n,j}^{(f)} - \bar{x}_n^{(f)}\right) \left(x_{n,j}^{(f)} - \bar{x}_n^{(f)}\right)^T. \quad (4)$$

Correspondingly, given the data vector d_n , we build a corresponding ensemble represented by the data matrix $d_n^{(e)}$ whose j^{th} -column is given by

$$d_{n,l}^{(e)} = d_n + \tilde{\epsilon}_{n,l}, \quad l = 1 \cdots N_e,$$

where the vectors $\tilde{\epsilon}_{n,j}$ are zero-mean Gaussian random vectors such that

$$\lim_{N_e \rightarrow \infty} \frac{1}{N_e - 1} \sum_{l=1}^{N_e} \tilde{\epsilon}_{j,l} \tilde{\epsilon}_{k,l}^T = \delta_{jk} R_k.$$

In the Ensemble Kalman Filter, the gain matrix K_n is still given by the formula above, but with the error covariance matrices given via Equation (4). This then allows for an analysis state, say $x_n^{(a)}$ ensemble-matrix approximation to be computed which is consistent with the classic Kalman filter in the linear, infinite ensemble number limit. To complete the recursive cycle then, we find the next ensemble-forecast matrix via

$$x_{n+1}^{(f)} = f\left(x_n^{(a)}\right).$$

Averages and approximate error covariance matrices are computed as above, and the Ensemble Kalman Filter cycle is continued.

Eularian Data Assimilation

In contrast to a Lagrangian approach, we focus on using Eularian measurements as the source of the data used in the Kalman filter. To do this, we suppose that we have at some set of fixed locations, say $x_j^{(p)}$, $j = 1 \cdots N_f$, pressure plates over which we obtain surface height measurements $\eta(x_j^{(p)}, t) + \epsilon_j^{(d)}(t)$. We likewise, using standard pseudo-spectral methods for solving the water-wave problem, have at any given time a numerically computed approximation to the surface, say $\tilde{\eta}(x, t)$, where

$$\tilde{\eta}(x, t) = \frac{1}{2K} \sum_{j=-K+1}^K (-1)^j \hat{\eta}_j e^{i\pi j x / L_x}, \quad x \in [-L_x, L_x].$$

Note, the scaling and sign choice are commensurate with the standard implementation of the Fast Fourier Transform in Matlab, NumPy, and so forth. Given the requirement that $\tilde{\eta}(x, t)$ is real, we have the symmetry constraint $\hat{\eta}_{-j} = \hat{\eta}_j^*$. For ease then, we set $\hat{\eta}_K = 0$, and note that the above representation for $\tilde{\eta}(x, t)$ can be rewritten as

$$\tilde{\eta}(x, t) = \frac{1}{2K} \left(\hat{\eta}_0 + 2 \sum_{j=1}^{K-1} (-1)^j \left(\text{Re}(\hat{\eta}_j) \cos\left(\frac{\pi j x}{L_x}\right) - \text{Im}(\hat{\eta}_j) \sin\left(\frac{\pi j x}{L_x}\right) \right) \right),$$

We therefore see that when comparing data to model forecasts, the observation operator $H = -\tilde{H}/K$, where \tilde{H} is given by the Vandermonde like matrix

$$\tilde{H} = \begin{pmatrix} 1/2 & c_{1,1} & \cdots & c_{1,(K-1)} & s_{1,1} & \cdots & s_{1,(K-1)} \\ 1/2 & c_{2,1} & \cdots & c_{2,(K-1)} & s_{2,1} & \cdots & s_{2,(K-1)} \\ \vdots & \vdots & \ddots & \vdots & \vdots & \ddots & \vdots \\ 1/2 & c_{N_f,1} & \cdots & c_{N_f,(K-1)} & s_{N_f,1} & \cdots & s_{N_f,(K-1)} \end{pmatrix}$$

where

$$c_{j,l} = (-1)^l \cos(l\tilde{x}_j), \quad s_{j,l} = (-1)^l \sin(l\tilde{x}_j)$$

with $\tilde{x}_j = \pi x_j^{(p)} / L_x$. Throughout the remainder of this section, we take the covariance matrices Q_n and R_n to be $\sigma^2 I$, where I denotes the identity matrix appropriate to the corresponding dimensionality of the random variable in question, and σ corresponds to the variance of the associated Gaussian random variables.

Data Assimilation

To generate the ‘true data’ which we will attempt to reconstruct, for $x \in [-L_x, L_x]$, we use the initial conditions

$$\begin{aligned}\eta_0(x) &= \frac{1}{E} \sum_{m=-K+1, \neq 0}^{K-1} e^{-(k_m - k_d)^2 / 2\tilde{\sigma}^2} e^{i(k_m x + \theta_m^{(\eta)})} \\ q_0(x) &= \frac{1}{E} \sum_{m=-K+1, \neq 0}^{K-1} e^{-(k_m - k_d)^2 / 2\tilde{\sigma}^2} e^{i(k_m x + \theta_m^{(q)})}\end{aligned}$$

where $\theta_{-m}^{(\eta, q)} = -\theta_m^{(\eta, q)}$, $k_m = \pi m / L_x$, and E is the l_2 normalization condition

$$E = \left(\sum_{m=-K+1, \neq 0}^{K-1} e^{-(k_m - k_d)^2 / \tilde{\sigma}^2} \right)^{1/2}.$$

The phases $\theta_m^{(\eta, q)}$ are randomly chosen from a uniform distribution over the interval $[0, 2\pi]$, and the $\neq 0$ means that both the initial surface and velocity potential have zero spatial mean. Throughout the remainder of this section we choose the primary direction of propagation, k_d , so that $k_d = \pi / L_x$. Thus, in the limit as $\tilde{\sigma} \rightarrow 0$, we go to the monochromatic initial conditions

$$\eta_0(x) \sim \cos\left(\frac{\pi}{L_x}x + \theta^{(\eta)}\right), \quad q_0(x) \sim \cos\left(\frac{\pi}{L_x}x + \theta^{(q)}\right), \quad \tilde{\sigma} \sim 0.$$

Note, our scaling choices ensure that each initial condition is $\mathcal{O}(1)$ in magnitude, which is consistent with the introduction of ϵ above as a measure of the effective surface-wave amplitude. To generate the high-order numerics, we use a pseudo-spectral scheme with $K_T = 2K = 256$ modes and a 4th-order Runge–Kutta scheme with an integrating factor and time step $dt = .01$. We take $\epsilon = .1$ and $\mu = \sqrt{\epsilon}$ since this is consistent with the scaling choices made to derive classic nonlinear shallow water models such as the Korteweg–de Vries equation. The number of terms used in the DNO expansion is $M = 14$, which generally ensures machine precision accuracy for relatively long time evolutions.

As for how we assimilate data, we set the number of ensemble members to be $N_e = 200$. To initialize the filter, we use the following initial conditions for $j = 1, \dots, N_e$

$$\eta_0^{(j)}(x) = \frac{1}{E} \sum_{m=-K+1, \neq 0}^{K-1} e^{-(k_m - k_d)^2 / 2\tilde{\sigma}^2} e^{i(k_m x + \theta_m^{(\eta, j)})}$$

$$q_0^{(j)}(x) = \frac{1}{E} \sum_{m=-K+1, \neq 0}^{K-1} e^{-(k_m - k_d)^2 / 2\tilde{\sigma}^2} e^{i(k_m x + \theta_m^{(q, j)})}$$

Note, by building our ensembles in this way, we are tacitly assuming that we know the initial power spectrum of the waves, leaving the only unknown to be the phases of each member of the ensemble. This assumption is consistent with the use of results from spectral-wave modeling to approximate the behavior of essentially random-sea states. Further, per our scaling choices, we have that the time scale $\tau_s = L/\sqrt{gH}$ is given by

$$\tau_s = \frac{L}{\sqrt{gH}} = \sqrt{\frac{H}{\epsilon g}} = \sqrt{H/1ms} = 10s, \quad H = 100m.$$

If we assume a relatively conservative sampling rate of 10 times per second, then we could choose a non-dimensional sampling rate of up to $dt_s = .05$, equal above to the time step of the numerical solver. However, this would not allow us to study the predictive power of our filtering process. Thus, we choose $dt_s = .5$, or a cycle of 5s between data assimilation events.

We likewise use a 4th-order Runge–Kutta scheme with an integrating factor in order to perform the analysis to forecast update. Each simulation is run up to $t_f = 20$, or about 200s, representing a reasonably realistic length of time. Lastly, we choose the magnitude of the covariance in the error associated with the data to be $\sigma = .1$. We note this value is an arbitrary choice in the Ensemble Kalman Filter, and should be chosen large enough to maintain invertibility in the computation of the gain matrix.

Eularian Data Assimilation Results

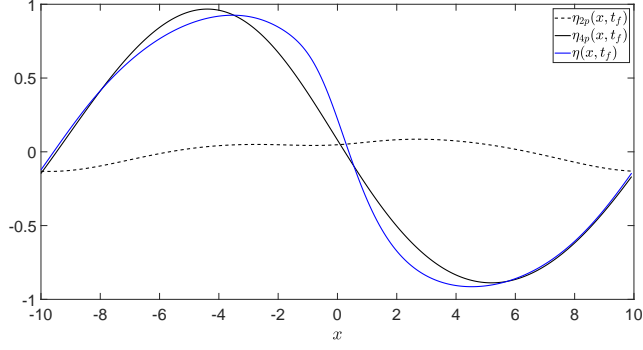
In the following figures, we look at comparisons between using two and four points of measurment as well as varying the degree of nonlinearity used in our modelling from $M = 0$ terms used in the DNO, corresponding to a stricly linear model, to $M = 1$, and then $M = 14$. Note, the error, $\mathcal{E}(t)$, is computed from the relative difference in the L_2 norm, i.e.

$$\mathcal{E}(t) = \frac{\|\eta_a(\cdot, t) - \eta_{tr}(\cdot, t)\|_2}{\|\eta_{tr}(\cdot, t)\|_2}.$$

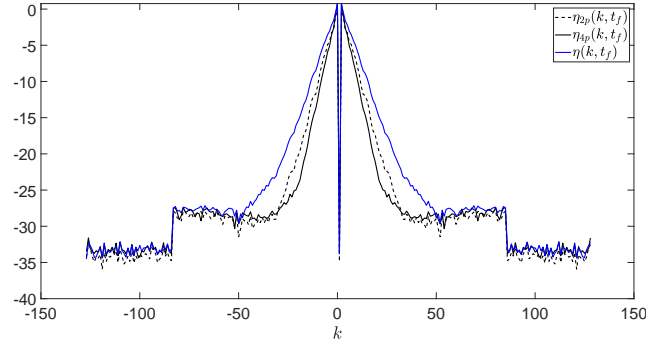
The results seen in Figures 1, 2, and 3 are in part as expected. Generally, four points of measurement is markedly better than two, and as seen in particular by comparing differences in power spectra, for the relatively long times, again $t_f = 20$, we run the simulations, the addition of nonlinearity to the model through the introduction of higher-order terms in the DNO improve accuracy.

However, what is perhaps surprising is the degree to which a relatively modest amount of nonlinearity enhances the overall accuracy of our assimilation/prediction approach; compare the two-point assimilation error in Figure 2 (c) to that in Figures 1 (c) and 3 (c). Thus it seems appropriate amounts of nonlinearity can potentially enhance otherwise unusable sparse measurement schemes.

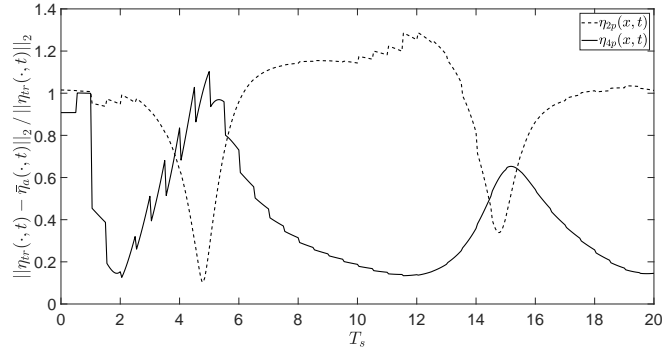
Of concern though is the common increase in error around $t = 15$ in each of the plots of $\mathcal{E}(t)$. To what extent this can be mitigated so that a more uniformly reliable assimilation/approximation scheme can be developed is question of ongoing research.



(a)



(b)

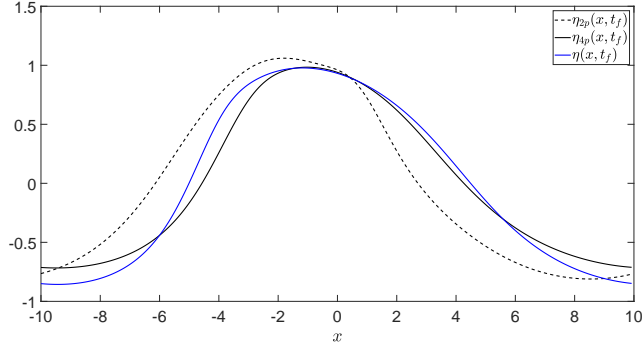


(c)

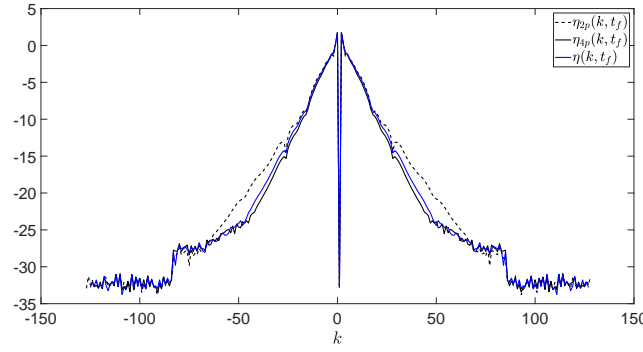
Figure 1: The pointwise-approximations (a) and power-spectrum approximations (b) at $t_f = 20$, and error (c) measuring at two (- -) and four points (-) using $M = 0$ terms in the DNO. The data-assimilation rate is $\delta t_s = .5$, so that the model is predicting behavior in between assimilation events.

References

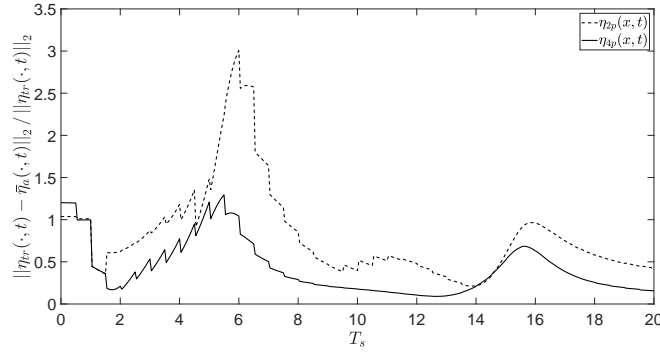
- [1] L. Kuznetsov, K. Ide, and C.K.R.T. Jones. A method for assimilation of Lagrangian data. *Mon. Wea. Rev.*, 131:2247–2260, 2003.



(a)



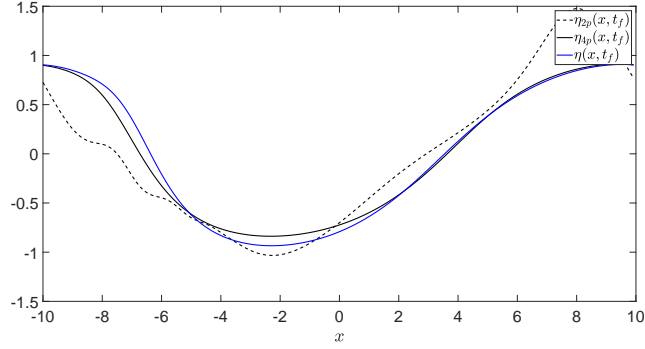
(b)



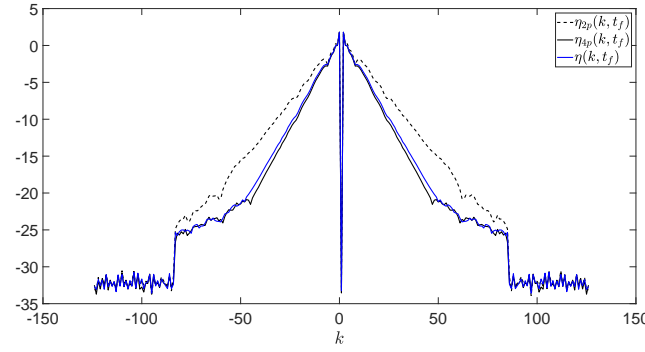
(c)

Figure 2: The pointwise-approximations (a) and power-spectrum approximations (b) at $t_f = 20$, and error (c) measuring at two (--) and four points (—) using $M = 1$ terms in the DNO. The data-assimilation rate is $\delta t_s = .5$, so that the model is predicting behavior in between assimilation events.

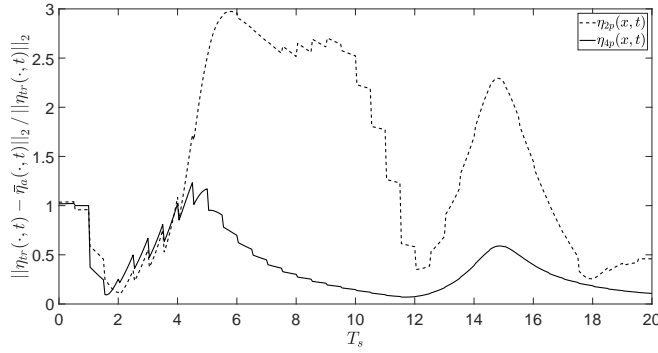
- [2] H. Salman, L. Kuznetsov, and C.K.R.T. Jones. A method for assimilating Lagrangian data into a shallow-water-equation ocean model. *Mon. Wea. Rev.*, 134:1081–1101, 2006.



(a)



(b)



(c)

Figure 3: The pointwise-approximations (a) and power-spectrum approximations (b) at $t_f = 20$, and error (c) measuring at two (--) and four points (—) using $M = 14$ terms in the DNO. The data-assimilation rate is $\delta t_s = .5$, so that the model is predicting behavior in between assimilation events.

- [3] A. Apte, C.K.R.T. Jones, and A.M. Stuart. A Bayesian approach to Lagrangian data assimilation. *Tellus*, 60:336–347, 2008.

- [4] L. Slivinski, E. Spiller, A. Apte, and B. Sandstede. A hybrid particle-ensemble Kalman filter for Lagrangian data assimilation. *Mon. Wea. Rev.*, 143:195–211, 2015.
- [5] E.T. Spiller, A. Apte, and C.K.R.T. Jones. Assimilating en-route Lagrangian observations. *Tellus*, 65:20319, 2013.
- [6] W. Craig and C. Sulem. Numerical simulation of gravity waves. *J. Comput. Phys.*, 108:73–83, 1993.
- [7] W. Craig, P. Guyenne, and H. Kalisch. Hamiltonian long-wave expansions for free surfaces and interfaces. *Comm. Pure Appl. Math.*, 58:1587–1641, 2005.
- [8] W. Craig, P. Guyenne, D. Nicholls, and C. Sulem. Hamiltonian long-wave expansions for water waves over a rough bottom. *Proc. R. Soc. A*, 461:839–873, 2005.
- [9] W. Craig, P. Guyenne, and C. Sulem. Water waves over a random bottom. *J. Fluid Mech.*, 640:79–107, 2009.
- [10] W. Craig and D. Nicholls. Travelling two and three-dimensional capillary gravity water waves. *SIAM J. Math. Anal.*, 32:323–359, 2000.
- [11] M.J. Ablowitz, A.S. Fokas, and Z.H. Musslimani. On a new non-local formulation of water waves. *J. Fluid Mech.*, 562:313–343, 2006.
- [12] K.L. Oliveras and V. Vasan. A new equation describing travelling water waves. *J. Fluid Mech.*, 717:514–522, 2013.
- [13] G. Evensen. The ensemble Kalman filter: theoretical formulation and practical implementation. *Ocean Dynamics*, 53:343–367, 2003.
- [14] E. Kalnay. *Atmospheric modeling, data assimilation, and predictability*. Cambridge University Press, Cambridge, 2003.
- [15] D.G. Dommermuth and D.K.P. Yue. A high-order spectral method for the study of nonlinear gravity waves. *J. Fluid Mech.*, 184:267–288, 1987.
- [16] J. Wilkening and V. Vasan. Comparison of five methods of computing the Dirichlet–Neumann operator for the water wave problem. In *Non-linear Wave Equations: Analytic and Computational Techniques*. AMS, 2015.
- [17] V.E. Zakharov. Stability of periodic waves of finite amplitude on the surface of a deep fluid. *Zhurnal Prikladnoi Mekhaniki i Tekhnicheskoi Fiziki*, 8:86–94, 1968.